Thermochimica Acta, 234 (1994) 103–125
Elsevier Science B.V., Amsterdam
SSDI 0040-6031(93)01503-U

Heat capacities and transitions in *n*-perfluoroalkanes and poly(tetrafluoroethylene)[1]

Y. Jin[a], A. Boller[a], B. Wunderlich[a,*] and B.V. Lebedev[b]

[a] *Department of Chemistry, The University of Tennessee, Knoxville, TN 37996-1600 (USA)* and *Division of Chemistry, Oak Ridge National Laboratory, Oak Ridge, TN 37831-6197 (USA)*

[b] *Chemistry Institute, N.I. Lobachevsky State University, Nizhny Novgorod (Russian Federation)*

(Received 26 November 1992; accepted 7 May 1993)

Abstract

Heat capacities and transitions of perfluorododecane ($C_{12}F_{26}$), perfluorotetradecane ($C_{14}F_{30}$), perfluorohexadecane ($C_{16}F_{34}$), perfluoroeicosane ($C_{20}F_{42}$) and perfluorotetracosane ($C_{24}F_{50}$) were measured by adiabatic calorimetry and differential scanning calorimetry from 5 K up to the melt. The heat capacities of the homologous series of perfluoroalkanes from *n*-octafluoropropane to poly(tetrafluoroethylene) in the solid state are analyzed using the Advanced THermal Analysis System (ATHAS) developed for linear macromolecules. All of the *n*-perfluoroalkanes show solid–mesophase transitions before the melting transition. The mesophases of short chain-length molecules can be identified as plastic crystalline (CF_4 to C_3F_8). After a group of intermediate length (C_4F_{10} to $C_{12}F_{26}$), the entropies of the solid–mesophase and isotropization transitions of the *n*-perfluoroalkanes approach the value of poly(tetrafluoroethylene) when expressed per mole of carbon atoms. Based on the measured heat capacities, it is possible to predict also the thermodynamic properties of the *n*-perfluoroalkanes not measured. Both disordering transition and isotropization temperature in the *n*-perfluoroalkanes with more than 12 carbon atoms can be expressed in functional form ($T_d = 295(n - 1.55)/(n + 7.55)$ and $T_i = 605(n - 3.56)/(n + 2.75)$, both in kelvin).

INTRODUCTION

Heat capacities of linear macromolecules has been a topic of long standing interest in our laboratory [1]. A major attempt was made to correlate all measured heat capacities by establishing a critically reviewed data bank [2]. Next, the heat capacities of the solid [3, 4] and liquid [5] states were interpreted in terms of their molecular motion. The analysis

---

* Corresponding author.

[1] Dedicated to Hans Georg Wiedemann.

was aided by the simplicity of linear molecules. The limits of this analysis were outlined in a prior publication [6]. In a previous paper, the feasibility of this analysis for shorter, linear molecules was explored by comparison of the heat capacities of polyethylene and *n*-alkanes [7]. It was found that the heat capacities of all *n*-alkanes with more than six carbon atoms can be represented by the contributions from group vibrations, known independently from IR and Raman spectra and from skeletal vibrations, described by Tarasov parameters (θ_1 and θ_3) which follow simple functions with molecular length. The analyses led to a precision of ±1.0%, which is similar to or better than that of most experimental determinations.

In the present paper earlier preliminary discussion on the interpretation of disorder in *n*-perfluoroalkanes [8] is to be extended, using all available literature data and new results. From the literature we collected heat capacities and information on transition for the following *n*-perfluoroalkanes: tetrafluoromethane (CF_4) [9], hexafluoroethane (C_2F_6) [10], perfluoropropane (C_3F_8) [11], perfluorobutane (C_4F_{10}) [12], perfluoropentane (C_5F_{12}) [13], perfluoro-hexane (C_6F_{14}) [14–16], perfluoroheptane (C_7F_{16}) [17], perfluorooctane (C_8F_{18}) [14, 15], perfluorodecane ($C_{10}F_{22}$) [18] perfluorododecane ($C_{12}F_{26}$) [15, 19, 20] perfluorotetradecane ($C_{14}F_{30}$) [21, 22], perfluorohexadecane ($C_{16}F_{34}$) [15, 20, 23], perfluoroeicosane ($C_{20}F_{42}$) [15, 19, 20, 24, 25], perfluorotetraeicosane ($C_{24}F_{50}$) [15], and poly(tetrafluoroethylene) (PTFE) [15, 26]. New measurements are presented for *n*-perfluorododecane ($C_{12}F_{26}$), perfluorotetradecane ($C_{14}F_{30}$), perfluorohexadecane ($C_{16}F_{34}$), perfluoroeicosane ($C_{20}F_{42}$) and perfluorotetraeicosane ($C_{24}F_{50}$).

With basic data on the heat capacity and transitions known, the equilibrium transitions and thermodynamic functions enthalpy (H) entropy (S) and Gibbs function (G) have been established and interpreted as a function of chain length. Short-chain *n*-perfluoroalkanes show a plastic crystalline meosphase before isotropization, whilst long-chain *n*-perfluoroalkanes show a conformationally disordered mesophase as is also seen in PTFE.

EXPERIMENTAL SECTION

Sample

Five *n*-perfluoroalkanes were studied: *n*-perfluorododecane ($C_{12}F_{26}$), *n*-perfluoro-tetradecane ($C_{14}F_{30}$), and *n*-perfluorohexadecane ($C_{16}F_{34}$) (obtained from PCR, Inc., Gainesville, FL), *n*-perfluoroeicosane ($C_{20}F_{42}$) and *n*-perfluorotetraeicosane ($C_{24}F_{50}$) (obtained from Aldrich Chemical Company, Inc., Milwaukee, WI). The samples were supplied with a purity of better than 98%.

Differential scanning calorimetry

A commercial Thermal Analysis 2100 System from TA Instruments Inc. with a 912 Dual Sample DSC and DSC Autosampler was used for heat capacity and transition measurements of all five samples. Experimental details and data analysis for heat capacity measurement were given in detail in previous papers [27–29]. A single-run heat capacity measurement technique was employed for the measurements [30]. The error is estimated to be <1% above 300 K and <2% between 200 and 300 K and <300 K and <3% below 200 K.

All heat capacities were measured at 10 K min^{-1} heating rate. Heat capacities were calibrated with a sapphire standard. Temperatures were calibrated at the transition temperatures of cyclopentane, cyclohexane, acetone, *n*-octane, naphthalene, indium and tin. Typical sample masses were 10–20 mg. The atmosphere in the calorimeter was nitrogen. All calorimeter placement was done with the Autosampler. Nonhermetic aluminum pans which are specially designed for the Autosampler were used for the C_p measurement from 130 to 330 K. Standard hermetic aluminum pans were used for transition measurement from 130 K to the melt, as well as for C_p measurement from 330 K to the melt since the samples will otherwise gradually sublime when the temperature is close to the melting point. Experimental error for the liquid C_p of the *n*-perfluoroalkanes might be more than 5% because of the sublimation.

Adiabatic calorimetry

Heat capacities of $C_{12}F_{26}$, $C_{14}F_{30}$ and $C_{16}F_{34}$ were also measured from 5 K to room temperature with an adiabatic vacuum calorimeter, described earlier [31]. The sample mass located in the calorimeter was about 1 g. The heat capacity of the samples was 60–70% of the total heat capacity of the calorimeter and the substance in the whole temperature interval. Here it should be repeated only that the calorimetric ampoule was a cylindrical vessel of platinum with a volume of approximately 15×10^{-6} m^3. The heat capacity of the ampoule increased smoothly from 0.028 to 4.420 J K^{-1} with rising temperature from 5 to 330 K. The temperature was measured with a platinum resistance thermometer ($R_0 = 52.0744\,\Omega$; $\alpha = 0.003258$). Liquid helium and nitrogen were used as cooling agents. The reliability of the calorimeter operation was tested by measuring heat capacities of standard corundum and benzoic acid. It was established by calibration with standards that the calorimeter and its procedure allows the heat capacity of the substance in the condensed state to be obtained within about 1% from 5 to 30 K, 0.5% in the range 30 to 50 K, and 0.2% between 50 and 320 K.

Calculation of heat capacities

The theory of heat capacity is well documented in several publications from our laboratory [3–6]. The computer programs for these calculations have been described in detail [3, 4]. In short, the heat capacity contributions of the group vibrations are computed making use of frequencies obtained from normal mode analyses coupled with IR and Raman data of *n*-perfluoroalkanes and PTFE. After subtracting the group vibration contributions from the experimental heat capacity at constant volume, C_V, the remaining skeletal contribution to the heat capacity is fitted with the two characteristic temperatures θ_1 and θ_3 of the Tarasov equation. Reversing this procedure, θ_1, θ_3 and the group vibrations permit the computation of the vibrational heat capacity at constant volume over a wide temperature range.

In somewhat more detail, the skeletal vibrations of linear macromolecules are approximated by the Tarasov model which consists of combination of one- and three-dimensional Debye functions and is given by [3]

$$C_V/NR = \mathrm{T}(\theta_1/T, \theta_3/T) = \mathrm{D}_1(\theta_1/T) - (\theta_3/\theta_1)[\mathrm{D}_1(\theta_3/T) - \mathrm{D}_3(\theta_3/T)] \quad (1)$$

where the one- and three-dimensional Debye functions D_1 and D_3 are represented by

$$C_V/NR = \mathrm{D}_1(\theta_1/T) = (T/\theta_1)\int_0^{(\theta_1/T)} \frac{(\theta/T)^2\exp(\theta/T)}{[\exp(\theta/T)-1]^2}\,\mathrm{d}(\theta/T) \quad (2)$$

$$C_V/NR = \mathrm{D}_3(\theta_3/T) = 3(T/\theta_3)^3\int_0^{(\theta_3/T)} \frac{(\theta/T)^4\exp(\theta/T)}{[\exp(\theta/T)-1]^2}\,\mathrm{d}(\theta/T) \quad (3)$$

T represents, as usual, the temperature in kelvin; R is the gas constant; N, the number of skeletal vibrations considered by the equation; and θ_1 and θ_3 are the upper frequency limits of the intra- and inter-molecular frequency distributions, expressed in kelvin (1 Hz = 8.40×10^{-11} K).

The group vibrations from narrow frequency distributions are represented by single Einstein functions E.

$$C_V/NR = \mathrm{E}(\theta_E/T) = \frac{(\theta_E/T)^2\exp(\theta_E/T)}{[\exp(\theta_E/T)-1]^2} \quad (4)$$

where θ_E is the Einstein frequency in K. Wider frequency ranges are averaged from an upper frequency θ_U to a lower frequency θ_L to compute the heat capacity contributions in a box distribution functions B.

$$C_V/NR = \mathrm{B}(\theta_U/T, \theta_L/T) = \frac{\theta_U}{\theta_U - \theta_L}[\mathrm{D}_1(\theta_U/T) - (\theta_L/\theta_U)\mathrm{D}_1(\theta_L/T)] \quad (5)$$

More complicated distributions are broken into several Einstein and box terms.

The conversion of the heat capacity at constant volume (C_V) to that at constant pressure (C_p) and vice versa is done by using a modified Nernst–Lindemann equation [32]

$$C_p - C_V = 3RA_0C_pT/T_m^\circ \tag{6}$$

where A_0 is a constant fitted to experimental data on compressibility and expansivity, or approximated by a universal value of 3.9×10^{-3} K mol J^{-1}; T_m° represents the equilibrium melting temperature. For the n-perfluoroalkanes discussed in this paper A_0 was taken to be 4.198×10^{-3} K mol J^{-1}, to agree with the limited experimental data of PTFE [32].

For long-chain n-perfluoroalkanes the skeletal vibrations (N in eqn. (1)) for each CF_2 group and CF_3 group are two and three, respectively, as establsihed in the prior polymer analyses. The number of group vibrations (N in eqns. (4) and (5)) for a CF_2 group is seven (one C–C stretching, two C–F stretching, and four C–F bending vibrations) and for a CF_3 group, N is nine (one C–CF_3 stretching, three C–F stretching and five C–F bending vibrations (the sixth bending vibration is related to the C–CF_3 torsional motion and for computational purpose is added to the skeletal vibrations)). For C_3F_8, as an example, the skeletal vibrations from one CF_2 and two CF_3 groups are 2 and 6, respectively. The group vibrations from two CF_3 groups are 18, and from one CF_2 group are 7. This counting was, however, developed for infinite chains. For the case of small molecules there is one less C–C stretching vibration which is now intermolecular between two C_3F_8 molecules and must be added to the skeletal vibrations. The other five intermolecular frequencies are properly accounted for in number by the Tarasov equation. The separation into inter- and intra-molecular vibration is also contained in the Tarasov analysis. Thus nine skeletal vibrations (six intermolecular and three intramolecular) and 24 group vibrations are needed for the heat capacity computation of C_3F_8.

The approximate group vibration frequencies of our calculations are listed in Table 1 and have been taken from data for PTFE [26] and hexafluoroethane (CF_3CF_3) [10, 33]. A comparison with similarly derived data for n-perfluoroalkanes shows little difference and would not significantly affect the calculated heat capacities [34].

Besides the calculation of heat capacities based on estimates of the skeletal and group vibrations, empirical addition schemes of heat capacities were used by assuming

$$C_p^{C_nF_{2n+2}}(T) = 2C_p^{CF_3}(T) + (n-2)C_p^{CF_2}(T) \tag{7}$$

for the heat capacities of solids and liquids. The liquid heat capacities

TABLE 1

Group vibration frequencies for n-perfluoroalkanes

Vibrational mode	N	Frequency/K [a]	C_nF_{2n+2}	C_3F_8
CF_2 (from PTFE)				
CF_2 asymm. stretching	0.67	1799, 2072	$(n-2)N$	0.67
	0.20	2085	$(n-2)N$	0.20
	0.13	1807	$(n-2)N$	0.13
CF_2 symm. stretching	0.17	1653	$(n-2)N$	0.17
	0.83	1040, 1660	$(n-2)N$	0.83
CF_2 bending	0.13	554	$(n-2)N$	0.13
	0.87	407, 554	$(n-2)N$	0.87
CF_2 wagging	0.20	829	$(n-2)N$	0.20
	0.20	906, 967	$(n-2)N$	0.20
	0.60	845, 967	$(n-2)N$	0.60
CF_2 twisting	0.23	423	$(n-2)N$	0.23
	0.77	273, 416	$(n-2)N$	0.77
CF_2 rocking	0.27	1086	$(n-2)N$	0.27
	0.73	442, 747	$(n-2)N$	0.73
C–C stretching	0.53	1670, 1984	$(n-3)N$	0.00
	0.47	1670, 1768	$(n-3)N$	0.00
Total	7.00		$7(n-2)-1$	6.00
CF_3 (from CF_3CF_3)				
CF_3 asymm. stretching	1.00	1799	$2N$	2.00
CF_3 asymm. stretching	1.00	1780	$2N$	2.00
CF_3 symm. stretching	1.00	2043	$2N$	2.00
C–CF_3 stretching	1.00	502	$2N$	2.00
CF_3 asymm. bending	1.00	752	$2N$	2.00
CF_3 symm. bending	1.00	892	$2N$	2.00
CF_3 rocking	1.00	1164	$2N$	2.00
CF_3 rocking	1.00	547	$2N$	2.00
Total	1.00	311	$2N$	2.00
	9.00		18	18.00
Total group vibrational modes			$7n+3$	24
Total skeletal vibrational modes			$2n+3$	9
Total vibrational modes			$3(3n+2)$	33
Total atoms in n-perfluoroalkanes			$3n+2$	11

[a] 1 Hz = 8.40×10^{-11} K.

change over wider temperature ranges linearly with temperature so that eqn. (7) can be written as

$$C_{p,\mathrm{liq.}}^{\mathrm{C}_n\mathrm{F}_{2n+2}}(T) = 2(\mathrm{A}^{\mathrm{CF}_3} + \mathrm{B}^{\mathrm{CF}_3}T) + (n-2)(\mathrm{A}^{\mathrm{CF}_2} + \mathrm{B}^{\mathrm{CF}_2}T) \qquad (8)$$

All data regressions were carried out by using Lotus 1-2-3® software.

RESULTS

Transitions

The transition behaviors of $C_{12}F_{26}$, $C_{14}F_{30}$, $C_{16}F_{34}$, $C_{20}F_{42}$ and $C_{24}F_{50}$ were studied by DSC on samples sealed in a hermetic pan (heated at a rate of 10 K min^{-1}). The DSC curves are summarized in Fig. 1. Before melting, with a high-temperature endotherm, all samples show one or two low-temperature transitions. At least three runs were carried out for each material, using the as-received samples. The average transition parameters are listed in Table 2 with the reference marked T and combined with literature data on all discussed *n*-perfluoroalkanes. The temperatures T_{d1}, T_{d2} and T_{d3} indicate multiple low-temperature transitions with corresponding entropies of transiton of ΔS_{d1}, ΔS_{d2} and ΔS_{d3}, respectively. The total disordering entropy $\Delta S_d = \Delta S_{d1} + \Delta S_{d2} + \Delta S_{d3}$ is also given. The melt is reached at the isotropization temperature T_i and ΔS_i is the corresponding entropy.

Figure 2 is a plot of the "best data" for the entropy of disordering and isotropization versus number of carbon atoms per *n*-perfluoroalkanes. Details of the evaluation of the "best data" are discussed below. Also given is the total entropy of fusion.

Heat capacity

The heat capacities of $C_{12}F_{26}$, $C_{14}F_{30}$, $C_{16}F_{34}$, $C_{20}F_{42}$ and $C_{24}F_{50}$ were measured by DSC, those of $C_{12}F_{26}$, $C_{14}F_{30}$ and $C_{16}F_{34}$ were also measured by adiabatic calorimeter. All data are listed in Table 3. Data for C_3F_8 and C_7F_{16} were available from the literature [11, 17].

The vibration-only heat capacity of C_3F_8, C_7F_{16}, $C_{12}F_{26}$, $C_{14}F_{30}$, $C_{16}F_{34}$,

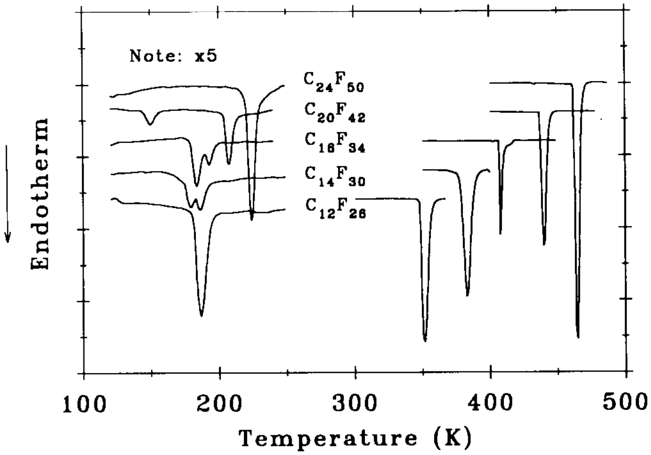

Fig. 1. The transitions as given by DSC curves of $C_{12}F_{26}$, $C_{14}F_{30}$, $C_{16}F_{34}$, $C_{20}F_{42}$ and $C_{24}F_{50}$.

TABLE 2

Transition temperatures in K and entropies in J K^{-1} mol^{-1} for *n*-perfluoroalkanes

	Mol. wt.	T_{d1}	T_{d2}	T_{d3}	ΔS_{d1}	ΔS_{d2}	ΔS_{d3}	ΔS_d	T_i	ΔS_i	Ref. (Method)
CF_4	88.005	76.2			22.6			22.6	89.6	7.9	9 (C)
C_2F_6	138.012	103.9			37.3			37.3	176.6	15.8	10 (C)
C_3F_8	188.020	99.3			35.6			35.6	125.4	3.8	11 (C)
C_4F_{10}	238.028	129			0.7			0.7	144	53.2	12 (D)
C_5F_{12}	288.036	144.5							147.5		13 (W)
C_6F_{14}	338.044	103			10.0			10.0	185	36.8	14 (C)
									182.5	49.4	15 (D)
									186.9	35.4	16 (W)
C_7F_{16}	388.051	180.5			36.9			36.9	221.8	31.3	17 (C)
										24.7	
C_8F_{18}	438.059	190	200					35.9	250	41.6	14 (C)
		175.6			18.0			18.0	254.2	37.7	15 (D)
$C_{10}F_{22}$	538.075	310									18 (?)
$C_{12}F_{26}$	638.090								347.6	69.0	19 (D)
		170.2			40.6			40.6	348.5	(109.6)	15 (D)
									348.2		20 (?)
		177.5	230.7		22.6	1.26		23.9			T (C)
		177.7			40.5			40.5	347.3	68.6	T (D)

$C_{14}F_{30}$	738.106	170.4	178.6		12.0	17.3		29.3			T (C)
		169.6	177.4		12.1	15.7		27.8	377.4	83.0	T (D)
									375		22 (?)
$C_{16}F_{34}$	838.122	170									23 (X)
		176.6	177.7	186.7	6.3	16.7	10.0	33.0	402.2	(152.3)	15 (D)
									398.2		20 (?)
		175.4	177.3	186.9	5.0	6.2	10.7	21.9			T (C)
		174.6		183.9	18.2		8.3	26.5	400.0	93.3	T (D)
$C_{20}F_{42}$	1038.153								435.6	105.6	19 (D)
		146	200						437		25 (D)
		149.5	202.9		4.2	55.6		59.8	437.9	(183.7)	15 (D)
		141.2	190.2						443.2	101.0	20 (?)
		150.8	200.0		9.0	50.0		59.0	436.9	122.5	T (D)
$C_{24}F_{50}$	1238.184	202.7			19.2			(19.2)	465.2	(217.1)	15 (D)
		217.5			64.4			64.4	461.7	136.8	T (D)
$(CF_2-)_n$	50.008	292	303		2.4	0.5		2.9	605	6.8	26 (D)
Virgin		292.2			2.4			2.4	619.5	8.2	15 (D)
Melted		292.2			3.0			3.0	601.7	7.7	15 (D)

Key: T, this work; (C), calorimetry; (D), DSC; (X), X-ray; (W), cooling and warming curves; (?) unknown.

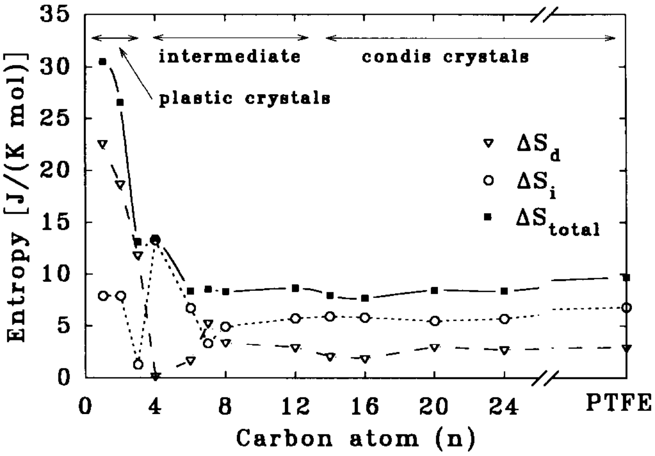

Fig. 2. Dependence of the transition entropies for disordering and melting transitions on chain length (calculated per mole of carbon atoms).

$C_{20}F_{42}$ and $C_{24}F_{50}$ were calculated based on an approximate vibrational spectra and θ values, fitted to experiment at low temperature, as outlined above. To obtain a good estimate of the limiting frequencies, heat capacities should be available in the temperature range of about 0.2θ to θ. For the n-perfluoroalkanes up to $C_{16}F_{34}$, heat capacity data were available from as low as 5 K so that both, θ_1 and θ_3 could be obtained. For the n-perfluoroalkanes $C_{20}F_{42}$ and $C_{24}F_{50}$, heat capacity data are available only above 100 K, so that only θ_1 could be obtained. The θ values of poly(tetrafluoroethylene) were evaluated similarly earlier [26]. Table 4 shows the θ values for the n-perfluoroalkanes and PTFE. An empirical relation between θ and chain length n, is given in Fig. 3. The value of θ_1 can be expressed by the following equation, derived for all n-perfluoroalkanes discussed in this paper and polytetrafluoroethylene:

$$\theta_1 = 250 - 281.6/n \qquad (n \geq 7) \tag{9}$$

A similar empirical plot of θ_3 versus $1/n$ is shown in Fig. 4. Due to the few data points, it is difficult to establish a secure correlation, but as a first approximation, a linear relation seems still to apply to n-perfluoroalkanes C_7F_{16} or longer. The values of θ_3 are expressed by the equation

$$\theta_3 = 54 - 98.5/n \qquad (n \geq 7) \tag{10}$$

Figure 5 shows the fit of the heat capacities between experiment (points) and calculation (lines) based on the θ values in Table 4 and the group vibration frequencies in Table 1. Figure 6 is a plot of the deviations of the vibration-only heat capacity calculation from the experiment.

TABLE 3

Experimental heat capacities for $C_{12}F_{26}$, $C_{14}F_{30}$, $C_{16}F_{34}$, $C_{20}F_{42}$ and $C_{24}F_{50}$ in J K^{-1} mol^{-1}

T/K	Adiabatic calorimetry			Differential scanning calorimetry				
	$C_{12}F_{26}$	$C_{14}F_{30}$	$C_{16}F_{34}$	$C_{12}F_{26}$	$C_{14}F_{34}$	$C_{16}F_{34}$	$C_{20}F_{42}$	$C_{24}F_{50}$
5	3.897	5.248	5.723					
10	21.98	24.26	26.32					
15	44.12	48.04	52.95					
20	65.47	72.19	80.35					
25	84.64	94.06	104.5					
30	101.6	113.2	125.8					
40	129.7	145.3	162.3					
50	153.5	173.2	193.1					
60	176.3	198.7	223.1					
70	199.3	222.2	253.2					
80	222.4	253.3	282.0					
90	245.3	275.7	312.3					
100	266.6	309.9	343.7					
110	288.5	329.5	373.8					
120	311.1	357.8	405.2	311.1	352.7	403.5	493.8	571.7
130	334.1	383.2	434.1	334.4	382.2	438.9	525.2	640.9
140	357.2	404.0	463.9	350.6	406.5	463.7	558.4	683.6
150	379.7	424.0	498.4	370.9	437.0	489.3	694.6	722.2
160	402.8	446.0	534.0	391.9	469.3	521.9	606.3	741.7
170	421.3	468.0	570.0	418.6	554.5	571.5	634.7	768.1
180	460.9	548.0	609.0	800.9	716.0	988.4	688.8	799.5
190	469.4	556.4	644.0	552.3	551.1	788.0	738.5	836.6
200	475.2	566.6	654.0	489.9	556.7	658.0	881.7	881.4
210	480.7	577.8	667.5	502.6	571.3	671.9	916.8	963.7
220	486.9	589.4	681.0	515.6	581.2	689.1	876.6	2345.6
230	493.7	602.2	693.5	530.7	592.4	704.4	895.9	1107.3
240	501.0	614.8	704.0	538.7	601.9	718.5	909.6	1095.4
250	508.4	627.4	714.8	550.5	612.3	733.7	924.6	1104.8
260	515.6	639.0	726.0	563.7	627.6	748.6	939.5	1114.1
270	522.8	651.0	738.0	576.1	642.0	761.8	951.3	1126.7
280	530.2	663.6	751.0	591.9	661.6	780.3	977.1	1140.5
290	538.6	680.8	763.0	609.5	672.4	795.8	1001.2	1155.5
298.15	546.8	691.6	772.5	620.3	679.3	809.7	1020.4	1169.3
300	548.9	694.0	775.0	623.8	684.7	813.8	1024.0	1174.1
310	562.6	707.6	786.0	646.1	707.2	833.1	1045.7	1193.7
320		722.4	797.5	670.0	727.0	850.0	1060.0	1220.0
330				705.0	747.0	870.0	1075.0	1250.0
340				734.7	775.1	880.0	1099.7	1279.9
350				4469.9	801.6	901.4	1116.4	1297.8
360				910.8	833.9	927.4	1137.1	1317.5
370				787.6	911.7	956.8	1163.1	1335.0
380				793.0	5029.5	994.8	1189.7	1360.4
390					1212.9	1057.8	1225.3	1394.9
400					925.4	1999.6	1270.2	1441.5
410					928.2	1596.8	1320.6	1489.8
420						1059.4	1376.6	1544.5
430						1060.2	1436.5	1593.0
440						1067.6	13549.4	1650.8
450							1390.7	1721.7
460							1372.7	1822.6
470							1382.4	2166.4
480								1623.9
490								1636.4
500								1643.7

TABLE 4

Tarasov parameters for *n*-perfluoroalkanes and PTFE [a]

n	$1/n$	θ_1/K	θ_3/K	N
3	0.333	148	60	9
7	0.143	210	40	17
12	0.083	227	48	27
14	0.071	230	47	31
16	0.063	232	48	35
20	0.050	235	(49)	43
24	0.042	240	(50)	51
PTFE	0.000	250	54	2

[a] Since the heat capacities of the short-chain molecules are given per mole of C_nF_{2n+2} and those of PTFE per mole of CF_2, care must be taken to use the proper N for the skeletal vibrational modes in the Tarasov equation (see Table 1 for the *n*-perfluoroalkanes and $N = 2$ for PTFE). The θ values were obtained by fitting experimental skeletal heat capacities to the Tarasov equation except for the data in parentheses, which were calculated from eqn. (10).

In addition to the detailed evaluation of the vibrational heat capacity, the CF_2 and CF_3 contributions to the heat capacities can be derived by empirical data regression analysis of all data. The results are shown in Fig. 7. A comparison of these data from the *n*-perfluoroalkanes and the heat capacity of PTFE is shown in Table 5. The quality of the C_p predictions

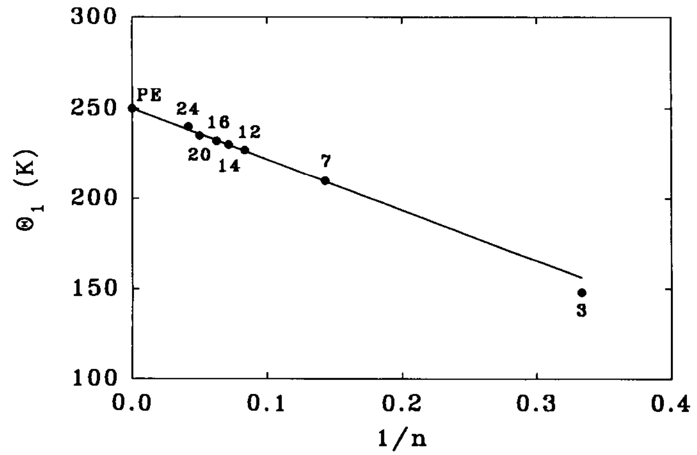

Fig. 3. Plot of θ_1 of C_3F_8 to $C_{24}F_{50}$ and PTFE vs. $1/n$. The line is represented by eqn. (9).

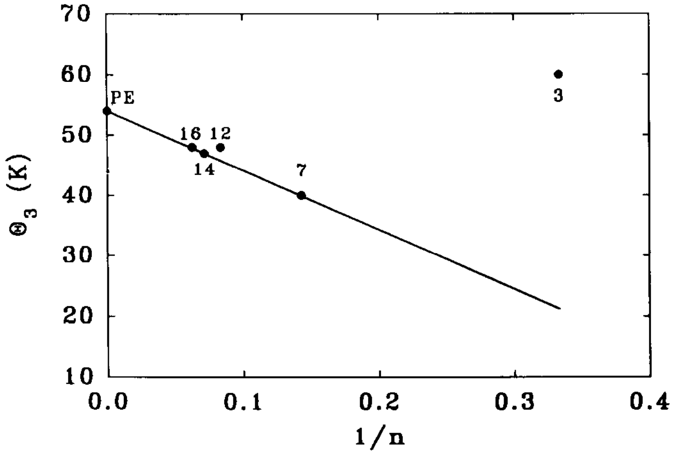

Fig. 4. Plot of θ_3 of C_3F_8 to $C_{16}F_{42}$ and PTFE vs. $1/n$. The line is represented by eqn. (10).

obtained by using calculation from the approximate frequency spectra and by the empirical addition schemes is summarized in Table 6.

DISCUSSION

Heat capacities and θ temperatures

The new measurements listed in Table 3 fit the common progression of heat capacities of a homologous series, as can be seen from Fig. 5. Although θ_3 for the calculation scheme was predicted from *n*-perfluoroalkanes of

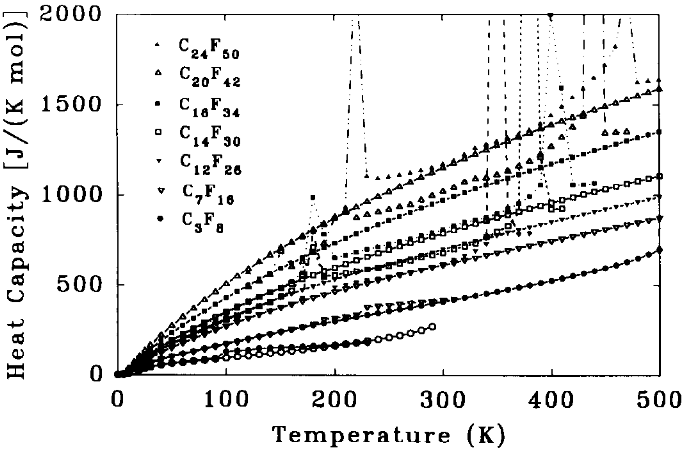

Fig. 5. Calculated (line) and experimental (symbols) heat capacities for C_3F_8 to $C_{24}F_{50}$.

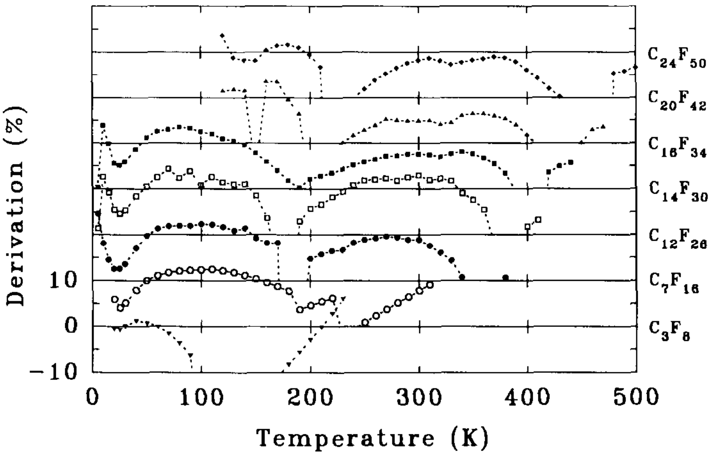

Fig. 6. Deviation between calculated and experimental heat capacity. Negative values indicate larger measured values.

only up to 16 carbon atoms (Fig. 4), the computed data for $C_{20}F_{42}$ and $C_{24}F_{50}$ agree with the measurements within the normally accepted experimental uncertainty of 1–3%. The ATHAS scheme is thus able to describe the heat capacity for all homologs with more than six carbon atoms, using the simple list of approximate group vibrations of Table 1 and the two characteristic temperatures, θ_1 and θ_3, given in eqns. (9) and (10). Figure 8 shows a typical comparison of measured and computed heat capacities for $C_{14}F_{30}$. The deviations of the experiments from the calculations at temperatures approaching the disordering transition and even in the mesophase up to 300–375 K are within typical error limits (see Fig. 6, C_7F_{16} to $C_{24}F_{50}$, respectively). For PTFE this deviation begins at about 500 K [26]. In all

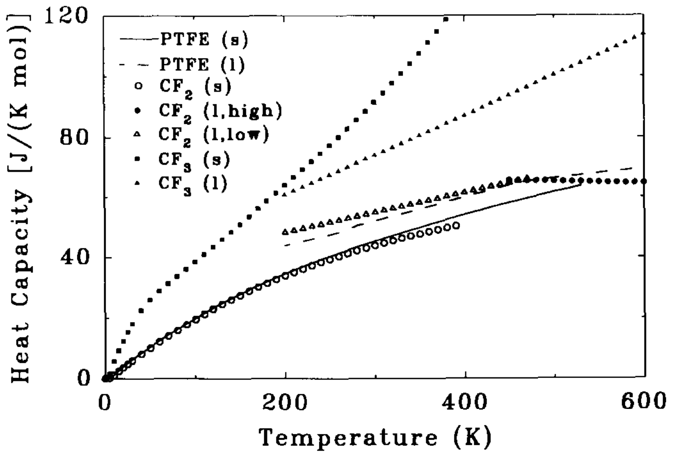

Fig. 7. Heat capacity contributions of CF_2 and CF_3 groups for liquids and solids.

TABLE 5

Heat capacity contributions of CF_2 and CF_3 groups from *n*-perfluoralkanes and PTFE in $J\,K^{-1}\,mol^{-1}$

T/K	Solid			T/K	Liquid			
	PTFE	*n*-Perfluoroalkanes			PTFE	*n*-Perfluoroalkanes		
	CF_2	CF_2	CF_3		CF_2	CF_2	CF_2	CF_3
5.00	0.22	0.16	1.47	200.00	43.86	48.44	67.39	60.77
10.00	1.29	1.12	5.64	210.00	44.61	49.10	67.32	62.10
15.00	2.65	2.42	9.16	220.00	45.35	49.76	67.26	63.42
20.00	3.95	3.65	12.32	230.00	46.10	50.41	67.19	64.75
25.00	5.18	4.82	15.30	240.00	46.86	51.07	67.13	66.07
30.00	6.35	5.94	18.04	250.00	47.61	51.73	67.06	67.40
40.00	8.54	8.08	22.62	260.00	48.37	52.39	67.00	68.72
50.00	10.57	10.12	26.06	270.00	49.13	53.05	66.93	70.05
60.00	12.53	12.11	28.86	273.15	49.37	53.25	66.91	70.46
70.00	14.44	14.05	31.38	280.00	49.89	53.70	66.87	71.37
80.00	16.32	15.95	33.76	290.00	50.66	54.36	66.80	72.70
90.00	18.17	17.82	36.12	298.15	51.28	54.90	66.75	73.77
100.00	19.97	19.62	38.51	300.00	51.42	55.02	66.73	74.02
110.00	21.71	21.35	40.96	310.00	52.19	55.68	66.67	75.35
120.00	23.37	23.01	43.44	320.00	52.97	56.68	66.60	76.67
130.00	24.98	24.60	54.96	330.00	53.74	56.99	66.54	78.00
140.00	26.51	26.10	48.50	340.00	54.52	57.65	66.47	79.32
150.00	27.98	27.55	51.06	350.00	55.30	58.31	66.41	80.65
160.00	29.41	28.94	53.64	360.00	56.09	58.96	66.34	81.97
170.00	30.77	30.26	56.21	370.00	56.87	59.62	66.28	83.30
180.00	32.10	31.54	58.80	380.00	57.66	60.28	66.21	84.62
190.00	33.38	32.77	61.40	390.00	58.45	60.94	66.15	85.95
200.00	34.61	33.95	64.00	400.00	59.25	61.59	66.08	87.27
210.00	35.81	35.09	66.61	410.00	60.04	62.25	66.01	88.60
220.00	36.98	36.19	69.25	420.00	60.84	62.91	65.95	89.92
230.00	38.12	37.27	71.90	430.00	61.64	63.57	65.88	91.25
240.00	39.24	38.32	74.59	440.00	62.45	64.22	65.82	92.57
250.00	40.32	39.31	77.31	450.00	63.25	64.88	65.75	93.90
260.00	41.36	40.27	80.06	460.00	64.06	65.54	65.69	95.22
270.00	42.39	41.21	82.86	470.00	64.87	66.20	65.62	96.55
273.15	42.71	41.50	83.75	480.00	65.39	66.85	65.56	97.87
280.00	43.42	42.14	85.70	490.00	65.72	67.51	65.49	99.20
290.00	44.42	43.03	88.60	500.00	66.05	68.17	65.42	100.52
298.15	45.21	43.72	91.02	510.00	66.38	68.83	65.36	101.85
300.00	45.50	43.89	91.57	520.00	66.71	69.49	65.29	103.17
310.00	46.37	44.74	94.61	530.00	67.05	70.14	65.23	104.50
320.00	47.32	45.56	97.72	540.00	67.38	70.80	65.16	105.82
330.00	48.26	46.36	100.92	550.00	67.71	71.46	65.10	107.15
340.00	49.18	47.13	104.21	560.00	68.04	72.12	65.03	108.47
350.00	50.08	47.86	107.61	570.00	68.37	72.77	64.97	109.80
360.00	50.97	48.57	111.13	580.00	68.71	73.43	64.90	111.12
370.00	51.84	49.25	114.78	590.00	69.04	74.09	64.83	112.45
380.00	52.69	49.89	118.57	600.00	69.37	74.75	64.77	113.77
390.00	53.52	50.50	122.53					
400.00	54.34	51.07	126.67					

TABLE 6

Error comparison between calculation and addition scheme

n	Error in solid/% [a]			Error in liquid/% [b]		
	T range/K	Average	R.m.s.	*T* range/K	Average	R.m.s.
3	20–70	−0.12	0.88	130–230	−0.51	0.24
7	20–170	−0.08	2.61	220–310	0.63	0.21
12	7–170	−0.97	3.10	370–380	−2.89	0.25
14	7–150	0.49	2.76	400–410	−0.85	0.42
16	7–160	−0.12	2.89	420–440	0.94	0.61
20	120–140	1.88	0.14	450–470	−0.66	0.57
24	120–200	0.49	1.76	480–500	0.28	0.44
PTFE[c]	30–250	0.61	1.87	560–700	–	0.20

[a] Error in solid based on calculation scheme. [b] Error in liquid based on addition scheme. [c] From ref. 26.

cases it leads directly into the fusion peak. The corresponding *n*-alkanes and polyethylene show similar deviations beginning at about 150, 200 and 290 K for similar chain lengths [7]. This higher temperature of the beginning of trans–gauche interchanges is in accord with the higher activation energy of the process in PTFE (18.5 versus 15 kJ mol^{-1}).

Since there are not enough data for odd *n*-perfluoroalkanes, we were unable to establish whether there is an odd/even effect in θ_3 as was found in the *n*-alkanes [7]. As in the *n*-alkanes [7], both θ_1 and θ_3 increase with chain length. The frequency θ_3 should be related to the upper frequency limit of the intermolecular vibrations. Its increase with chain length must be an indication of an overriding increase in intermolecular forces, since the effect of the increase in molecular mass would result in a decrease in

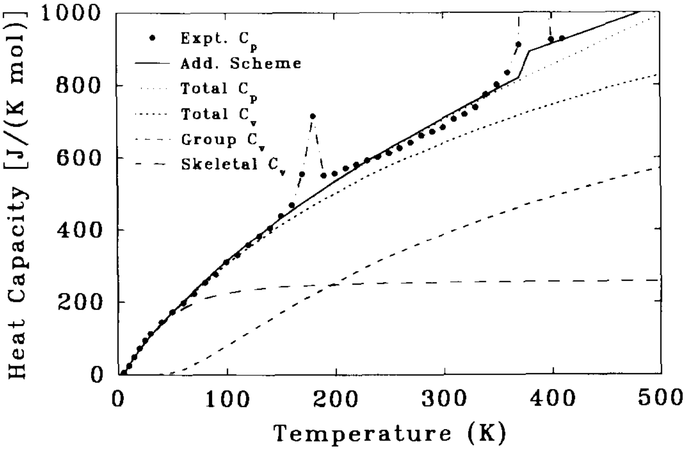

Fig. 8. Heat capacities of $C_{14}F_{30}$ from calculation, experiment, and addition schemes.

limiting frequency. On a percentage base, the change in frequency θ_3 in going from seven carbons to infinity is similar for *n*-alkanes and *n*-perfluoroalkanes (32% and 26%, respectively). The increase in θ_1 from C_7 to C_∞ is 19% and 16% for the *n*-alkanes and *n*-perfluororalkanes, respectively. As pointed our earlier, it is difficult to establish the actual vibration involved in the maximum of the intramolecular vibrations θ_1 due to coupling with group vibrations [6]. The increase in frequency is most likely linked to a stiffening of the lamellae, as proposed for the *n*-alkanes [7]. The upper limit of the frequency of the longitudinal acoustic mode (LAM) should, as in polyethylene, be more or less constant with chain length.

Addition schemes for heat capacities

Besides the more detailed linkage of heat capacity to approximate vibrational spectra, an effort is also made in our ATHAS to develop purely empirical addition schemes based on group contributions of chain elements, as given by eqns. (7) and (8) [35, 36]. This treatment is particularly useful for the description of liquid heat capacities.

Table 5 and Fig. 7 display the data regression results for the CF_2 and CF_3 groups from solid and liquid C_p data. In the solid state, the heat capacity of PTFE is practically identical to that of the perfluoroparaffinic CF_2 group. Unlike for the *n*-alkanes, we were unable to get a good regression result for the liquid *n*-perfluoroalkanes using a single linear equation. The heat capacity of liquid PTFE, however, shows also a break at 470 K [26], resulting in a lower heat capacity at low temperature than extrapolated linearly from measurement in the molten state. Assuming a similar change of C_p with temperature we separated the *n*-perfluororalkanes into two groups (C_3F_8 to $C_{16}F_{34}$ and $C_{20}F_{42}$ to $C_{24}F_{50}$) for data regression. For the group of small chain length, the CF_2 and CF_3 contributions to the heat capacity can be described by the equations

$$C_p^{CF_2} = 35.29 + 0.06576T \tag{11}$$

$$C_p^{CF_3} = 34.27 + 0.1325T \tag{12}$$

where data from T from 130 to 440 K were included in the regression, and C_p is given in J K^{-1} mol^{-1}. For the longer chain lengths, due to the few data points, one can get only approximate results. Assuming the CF_3 contribution is the same for all *n*-perfluoroalkanes one can estimate the CF_2 contribution for this group to be

$$C_p^{CF_2} = 68.70 - 0.006551T \tag{13}$$

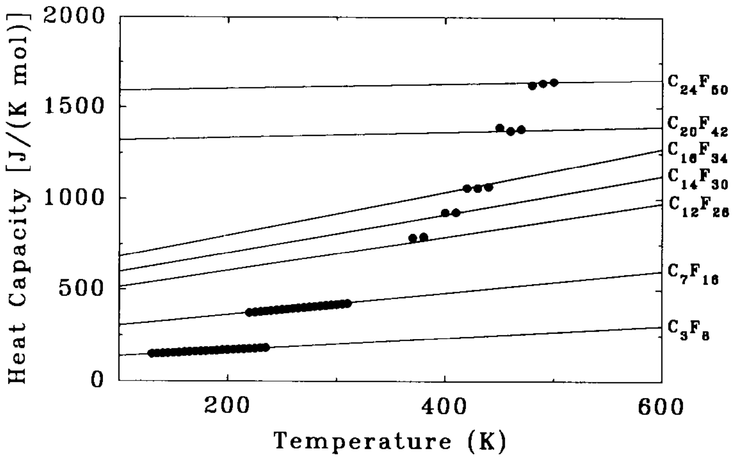

Fig. 9. Computed and measured heat capacities of the liquid *n*-perfluoroalkanes. The two upper curves are represented by eqns. (11) and (12) and the five lower curves by eqns. (12) and (13).

where data for T from 450 to 500 K were included in the regression, and C_p is given in J K^{-1} mol^{-1}. The break in linearity for the heat capacity contribution for the *n*-perfluoroalkanes can be seen to occur also at about 470 K. To estimate the heat capacity of liquid *n*-perfluoroalkanes we should thus use eqn. (11) up to 470 K and eqn. (13) above 470 K in eqn. (7). Equation (12) applies to the whole temperature range. The agreement between *n*-perfluororalkanes and PTFE might be improved if more data were available with better precision. Figure 9 shows computed and measured heat capacities of the liquid *n*-perfluoroalkanes. Practically all heat capacities of liquid *n*-perfluoroalkanes can thus be predicted. Typical errors are displayed in Table 6.

Transitions and motion

The newly measured transition behavior of $C_{12}F_{26}$, $C_{14}F_{30}$, $C_{16}F_{34}$, $C_{20}F_{42}$ and $C_{24}F_{50}$ agrees reasonably well with those of refs. 19, 20 and 24, but some of the entropies of transitions disagree significantly with those of ref. 15. The reason for the discrepancy could not be resolved. At present, the most reasonable explanation has to be a systematic error, perhaps in the quality of the samples or their crystallization history.

Unlike *n*-alkanes which may have disordering transitions very close to the isotropization temperature, or even have none, all *n*-perfluoroalkanes have one or more disordering transitions much below the isotropization temperature. For the following discussion a "best data" set has been

TABLE 7

"Best data" of transition entropies for *n*-perfluoroalkanes in $\mathrm{J\,K^{-1}\,mol^{-1}}$ [a]

Compound	ΔS_d		ΔS_i		ΔS_{total}	
	Per molecule	Per C atom	Per molecule	Per C atom	Per molecule	Per C atom
CF_4	22.6	22.6	7.9	7.9	30.5	30.5
C_2F_6	37.3	18.7	15.8	7.9	53.1	26.6
C_3F_8	35.6	11.9	3.8	1.3	39.4	13.1
C_4F_{10}	0.7	0.2	53.2	13.3	53.9	13.5
C_5F_{12}						
C_6F_{14}	10.0	1.7	40.3	6.7	50.3	8.4
C_7F_{16}	36.9	5.3	23.0	3.3	59.9	8.6
C_8F_{18}	27.0	3.4	39.6	5.0	66.6	8.3
C_9F_{20}						
$C_{10}F_{22}$						
$C_{11}F_{24}$						
$C_{12}F_{26}$	35.0	2.9	68.8	5.7	103.8	8.7
$C_{13}F_{28}$						
$C_{14}F_{30}$	28.6	2.0	83.0	5.9	111.6	8.0
$C_{15}F_{32}$						
$C_{16}F_{34}$	27.1	1.7	93.3	5.8	123.1	7.7
$C_{17}F_{36}$						
$C_{18}F_{38}$						
$C_{19}F_{40}$						
$C_{20}F_{42}$	59.4	3.0	109.7	5.5	169.1	8.5
$C_{21}F_{44}$						
$C_{22}F_{46}$						
$C_{23}F_{48}$						
$C_{24}F_{50}$	64.4	2.7	136.8	5.7	201.2	8.4
$(CF_2\text{–})_n$	2.9	2.9	6.8	6.8	9.7	9.7

[a] Average using all except the data of ref. 15 shown in parentheses in Table 2.

derived in Table 7 from the results of Table 2 by taking averages of all but the data in parentheses of Table 2. The lines in Fig. 2 are drawn to fit the data of Table 7.

For the rigid molecules CF_4, C_2F_6 and C_3F_8, the value of ΔS_d is within the range established for a crystal to plastic crystal transition (20–50 $\mathrm{J\,K^{-1}\,mol^{-1}}$) [8]. Since ΔS_d for plastic crystals is largely size independent (C_{60} has a ΔS_d of 27.3 $\mathrm{J\,K^{-1}\,mol^{-1}}$ at 256.1 K [37]), the plot of Fig. 2 shows a rapidly decreasing ΔS_d calculated per mole of carbon atoms.

The entropy of isotropization of these short-chain molecules corresponds approximately to the expected residual positional disordering entropy (ΔS_f for molecules of spherical shape, 7–14 $\mathrm{J\,K^{-1}\,mol^{-1}}$) [8]. The extraordinarily low value of C_3F_8 may be an indication of large translational diffusion in the plastic crystalline phase, a not uncommon observation.

The transition behavior of the next homologs C_4F_{10} to about $C_{10}F_{22}$ is intermediate between the long-chain molecules and the short-chain molecules. Table 7 shows that from perhaps $C_{12}F_{26}$ a similarity to PTFE can be detected. The disordering in PTFE has been linked to a dynamic disordering of left-handed and right-handed helix conformations (conformationally disordered crystal, in short, condis crystal) [26]. At low temperature, the stable triclinic crystal has a 1*13/6 helix that, after a minor transition at 292 K to a trigonal crystal with a 1*15/7 helix, changes, at 303 K, to the pseudohexagonal condis crystal. The relatively low entropy of disordering of 2.9 J K^{-1} mol^{-1} of CF_2 is comparable to the disordering of *n*-alkanes from C_9H_{20} to $C_{36}H_{74}$ to the hexagonal, so-called "rotor phase" (2.4–3.4 J K^{-1} mol^{-1} of CH_2). Recent molecular dynamics simulations [38] of full crystals of *n*-alkanes have given a better understanding of the "rotation" of the chains that yields the average hexagonal symmetry. On a nanometer scale domains of the low-temperature structure can be seen at any instant with considerable packing defects. The size, boundary, and orientation of the domains changes continuously on a picosecond timescale by a twist-motion of the chains with amplitudes of rotation between consecutive CH_2 groups of less then 90°. This dynamic defect structure presents an averaged, highly symmetric structure to the X-ray analysis. For polyethylene a hexagonal phase is stable, except for special conditions, only at elevated pressure and temperature. It has, in contrast to the *n*-alkanes and *n*-perfluoroalkanes, a high percentage of gauche conformations (rotation about the C–C bond by about 120°). The gauche concentration has been estimated to be close to 40%, the value expected for the melt [8]. Naturally its ΔS_d is, due to the need to introduce the gauche conformations, larger than that of the *n*-alkanes and *n*-perfluoroalkanes. It was estimated to be 7.1 J K^{-1} mol^{-1} at 520 K and 500 MPa. The *n*-alkanes in their hexagonal phase, in contrast, show at most a few percent gauche bonds, sufficient however, to cause a clearly observable increase in heat capacity beyond the value due to vibrations only. The disordered phase of PTFE does not seem to collect any significant gauche conformation until approaching the isotropization temperature and keeps the chain largely librating in the two minima expected close to the trans conformation [39]. The isotropization entropy of 6.8–8.2 J K^{-1} mol^{-1} of Table 2 is in agreement with close to one bond per CF_2 becoming conformationally disordered at T_i. Typical values for the conformational entropy of disordering are 7–14 J K^{-1} mol^{-1} [8]. For the *n*-perfluoroalkanes $C_{12}F_{26}$ and longer, one can describe thus, the hexagonal phase as mainly librating in the trans double-well potential causing rotations of the chain by segmental twist.

The intermediate *n*-perfluoroalkanes start with C_4F_{10}. Its "disordering" is almost negligible and could even be accounted for by a change in crystal structure without a large increase in mobility. The next members of the series show an increase in ΔS_d to reach a maximum at C_7H_{16}, then decrease to a constant value at about $C_{12}F_{26}$. It may well be that these chains, being too short to form a full helix within their molecular length, show still some rotational motion of the molecule as a whole. Because of the geometry of the chain the motion could only be about one axis. This restricted rotation must have a lower ΔS_d than that of a plastic crystal transition. The value is increased, however, by additional segmental mobility (libration), and decreased by a change to jump-like motion.

Enthalpy, entropy and free enthalpy

With heat capacities either known or predictable for all *n*-perfluoroalkanes, it is possible to establish the complete thermodynamic functions as soon as all transition parameters are determined. From the present work complete tables for enthalpy, entropy, and free enthalpy have been computed for the perfluoroalkanes discussed in this paper. Data tables for any of the *n*-alkanes, as well as polyethylene and the other more than 100 polymers that are part of the ATHAS Data Bank can be requested from the authors. A typical example is shown in Fig. 10 for the *n*-perfluorotetradecane ($C_{14}F_{30}$).

Isotropization and disordering temperature

With the high probability that the isotropization temperatures of the *n*-perfluoro-alkanes above $C_{13}F_{28}$ refer to similar crystal structure and motional states as in PTFE, an attempt can be made to try to express T_i as a

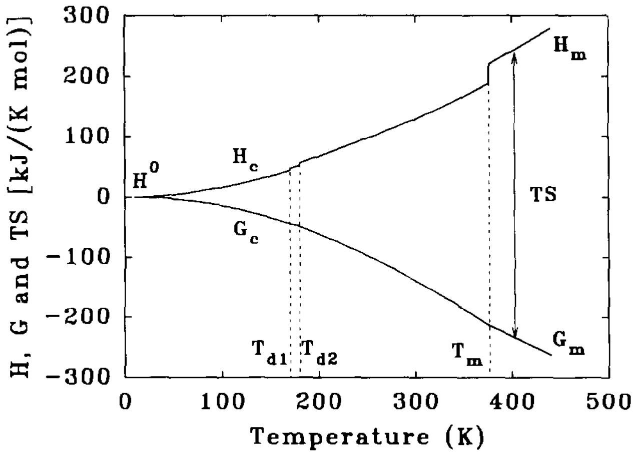

Fig. 10. Thermodynamic functions for *n*-perfluorotetradecane ($C_{14}F_{30}$). Note that $H - G = TS$.

function of chain length. The experimental data of Table 2 have a typical experimental error of ±(0.5 to 3) K. Averages of all reported isotropization temperatures can be fitted to the equation

$$T_i = 605 \frac{n - 3.56}{n + 2.75} \tag{14}$$

Equation (14) reproduces the averages of T_i for $C_{14}F_{30}$ to $C_{24}F_{50}$ with an error of ±1.0 K. The empirical eqn. (14) is similar to one derived for *n*-alkanes, and can be used to fix the isotropization temperature for the not measured homologs.

To use a similar expression for the disordering transitions, the close lying multiple transition temperatures were averaged and the minor T_{d1} for $C_{20}F_{50}$ omitted. This led to experimental data with typical deviations of ±5 K. The equation

$$T_d = 295 \frac{n - 1.55}{n + 7.55} \tag{15}$$

represents the average experimental data with an error of about ±2.5 K.

With heats of transition as well as temperatures of transition known, a full characterization is possible for all *n*-perfluoroalkanes from $C_{13}F_{28}$ to PTFE.

CONCLUSIONS

This research has completed the thermodynamic characterization of a second series of homologous compounds from the monomer to the polymer. A prediction of heat capacities from C_6 to the macromolecule is possible. The hexagonal phase of the fluoropolymers is linked to that of the hexagonal phase of *n*-alkanes and contrasted to that to the hexagonal phase of polyethylene at high temperature and pressure. A small heat capacity increase before the disordering transitions is thought, as in the *n*-alkanes, to arise from a small amount of conformational disorder. The transitions for molecules with more than twelve carbon atoms can be fully characterized by using empirical equations for the disordering and isotropization temperatures, and measured transition enthalpies that change only little when expressed per mole of carbon atom.

ACKNOWLEDGMENT

This work was supported by the Division of Materials Research, National Science Foundation, Polymers Program, Grant DMR 92-00520 and the Division of Materials Sciences, Office of Basic Energy Sciences, U.S. Department of Energy, under Contract DE-AC05-84OR21400 with Martin Marietta Energy Systems, Inc.

REFERENCES

1 B. Wunderlich and M. Dole, J. Polym. Sci., 24 (1957) 201.
2 The ATHAS Data Bank 1980: U. Gaur, S.-F. Lau, H.-C. Shu, B.B. Wunderlich, A. Mehta and B. Wunderlich, J. Phys. Chem. Ref. Data, 10 (1981) 89, 119, 1001; 11 (1982) 313, 1065; 12 (1983) 29, 65, 91. Update 1990: M. Varma-Nair and B. Wunderlich, J. Phys. Chem. Ref. Data, 20 (1991) 349.
3 Yu.V. Cheban, S.-F. Lau and B. Wunderlich, Colloid Polym. Sci., 260 (1982) 9.
4 S.-F. Lau and B. Wunderlich, J. Therm. Anal., 28 (1983) 59.
5 K. Loufakis and B. Wunderlich, J. Phys. Chem., 92 (1988) 4205.
6 H.S. Bu, S.Z.D. Cheng and B. Wunderlich, J. Phys. Chem., 91 (1987) 4179.
7 Y. Jin and B. Wunderlich, J. Phys. Chem., 95 (1991) 9000.
8 B. Wunderlich, M. Möller, J. Grebowicz and H. Baur, Conformational Motion and Disorder in Low and High Molecular Mass Crystals, Adv. Polymer Sci., Vol. 87, Springer Verlag, Berlin, 1988, pp. 50–54, 84, 85.
B. Wunderlich and J. Grebowicz, Adv. Polymer Sci., 60/61 (1984) 1.
9 J.H. Smith and E.L. Pace, J. Phys. Chem., 73 (1969) 4232.
10 E.L. Pace and J.G. Aston, J. Am. Chem. Soc., 70 (1948) 566.
11 E.L. Pace and A.C. Plaush, J. Chem. Phys., 47 (1967) 38.
12 M. Campos-Vallettee and M. Rey-Lafon, J. Mol. Struct., 101 (1983) 23.
13 J.H. Simon and R.D. Dunlap, J. Chem. Phys., 18 (1950) 335.
14 M. Campos-Vallettee, M. Rey-Lafon and R. Lagnier, Chem. Phys. Lett., 89 (1982) 189.
15 H.W. Starkweather, Jr., Macromolecules 19 (1986) 1131.
16 R.D. Dunlap, J.C. Murphy and R.C. Bedford, J. Am. Chem. Soc., 80 (1958) 83.
17 G.D. Oliver and J.W. Grisard, J. Am. Chem. Soc., 73 (1951) 1688.
18 J.F. Rabolt, T.R. Russell and R.J. Tweig, Macromolecules, 17 (1984) 2786.
19 P. Smith and K.H. Gardner, Macromolecules, 18 (1985) 1222.
20 H. Segwichert, Dissertation, Johannes Gutenberg University, Mainz, Germany, 1984.
21 G.W. Chantry, E.A. Nicol, R.G. Jones, H.A. Willis and M.E.A. Cudby, Polymer, 18 (1977) 37.
22 R.J. Twieg and J.F. Rabolt, Macromolecules, 21 (1988) 1806.
23 C.W. Bunn and E.R. Howells, Nature, 174 (1954) 549.
24 G.R. Strobl, H. Schwickert and T. Trzebiatowski, Ber. Bunsenges. Phys. Chem., 87 (1983) 274.
25 H. Schwickert, G. Strobl and M. Kimig, J. Chem. Phys., 95 (1991) 2800.
26 S.-F. Lau, H. Suzuki and B. Wunderlich, J. Polym. Sci. Polym. Phys. Ed., 22 (1984) 379.
27 Y. Jin and B. Wunderlich, J. Therm. Anal., 36 (1990) 765.
28 Y. Jin and B. Wunderlich, J. Therm. Anal., 36 (1990) 1519.
29 Y. Jin and B. Wunderlich, J. Therm. Anal., 1992, 38 (1992) 2257.
30 B. Wunderlich, J. Thermal Anal., 32 (1987) 1949.
31 B.V. Lebedev, T.G. Kulagina and N.N. Smirnova, J. Chem. Thermodyn., 20 (1988) 1383.
32 R. Pan, M. Varma-Nair and B. Wunderlich, J. Therm. Anal., 35 (1989) 955.
33 E.L. Pace, A.C. Plaush and H.V. Samuelson, Spectrochim. Acta, 22 (1966) 993.
34 H.-G. Cho, H.L. Strauss and R.G. Snyder, J. Phys. Chem., 96 (1992) 5290.
35 U. Gaur, M.-Y. Cao, R. Pan and B. Wunderlich, J. Therm. Anal., 31 (1986) 421.
36 R. Pan, M.-Y. Cao and B. Wunderlich, J. Therm. Anal., 31 (1986) 1319.
37 Y. Jin, J. Cheng, M. Varma-Nair, G. Liang, Y. Fu, B. Wunderlich, X.-D. Xiang, R. Motovoy and A.K. Zettl. J. Phys. Chem., 96 (1992) 5151.
38 (a) G.L. Liang, D.W. Noid, B.G. Sumpter and B. Wunderlich, Makromol. Chemie Theory and Simulation, 2 (1993) 245.
(b) L. Liang, D.W. Noid, B.G. Sumpter and B. Wunderlich, Acta Polym., 44 (1993) 219.
39 T.W. Bates, Trans. Faraday Soc., 63 (1967) 1825.